WrapToR composite truss structures: Improved process and structural efficiency

*Christopher John Hunt, Michael R. Wisnom and Benjamin King Sutton Woods

Bristol Composites Institute (ACCIS), Department of Aerospace Engineering, University of Bristol, United Kingdom, BS81TR

*Email: chris.hunt@bristol.ac.uk

ABSTRACT

Wrapped Tow Reinforced (WrapToR) trusses are ultra-efficient composite structural members that are produced using a novel winding process. In this study, a novel technique is employed during the manufacturing process to improve structural efficiency. By twisting the fibre tow bundle during winding, more consistent shear members were produced that displayed improved buckling resistance. Results from a three-point bend test showed this technique to increase truss failure load by 51 % for a particular truss size that is prone to shear web buckling. Comparison of experimental deflections to a previously developed structural analysis tool highlight the importance of capturing deflections due to shear loading. Finally, the truss configuration is experimentally compared to commercially available carbon fibre tubes. When compared to an 8 mm pultruded tube, the truss configuration displayed 9 % lower mass, over double the load carrying capability and 6.7 times the flexural rigidity.

Keywords: Composite truss structure, Filament winding, Mechanical testing, Buckling

1 Introduction

For the designer, two options are available to improve efficiency of a load bearing structure: change the material, or change the geometry [1]. A key characteristic of an efficient geometry is that it disperses material away from the axes of bending or torsion. When using simple prismatic section beams such as tubes, boxes or I-beams, maximum efficiency is restricted by practical limits of minimum material thickness which come from both manufacturing constraints and failure mechanisms, such as local buckling and plastic collapse [2]. Trusses and space frames are structures formed of multiple individual elements connected at joints that are able to surpass the efficiency limits of simple sections. By grouping material together into localised, discrete elements, they can move material further from the axis of bending or torsion while avoiding failure mechanisms associated with insufficient material thickness. Further efficiency gains are also achieved as the elements that make up such structures carry primarily axial loads, meaning material within each element is loaded equally [3], [4].

Owing to their impressive specific properties, advanced composite materials are an increasingly common choice for improving structural efficiency. While these materials are now utilised in a wide range of applications, their use is most beneficial in applications where there is a primary stress direction and where that direction is known. In these applications the anisotropic nature of composites can be exploited to maximise material properties in the dominant stress direction by aligning the fibres.

As loading within truss members is dominant along their length, forming these members of fibre reinforced composites would seem intuitive. Not only would this result in a combination of highly efficient geometry and material, aligning fibres with the members length would maximise material properties in the primary stress direction. Implementing composites within truss structures has therefore been highlighted as a means of maximising the potential benefits that fibre reinforced materials offer [5]. Despite this, the use of composite trusses to date has been limited. A possible reason for this is that manufacturing of traditional trusses requires joining together many individual members. While this has a significant impact on manufacturing difficulty, and therefore cost, for all types of trusses, it poses even more of a challenge when using composites as creating joints between composite parts is notoriously difficult. One example that perhaps highlights this issue is the CFRP truss developed by Schütze [6] and used in the Zeppelin NT airship structure. To achieve sufficient adhesion between elements, nodal gusset plate connectors made from CFRP were manufactured and used at each joint. While the CFRP truss concept offered a mass reduction of over 50 % compared to an aluminium equivalent, the manufacturing process involved production and assembly of a huge number of composite parts, making it unsuitable for many industrial applications.

Some researchers have investigated producing composite trusses using novel manufacturing techniques that reduce or remove the need for bonding multiple members. Such techniques are often created by modifying well-known composite manufacturing processes. Studies by Xiong et al. [7] and Li et al. [8] used modified versions of the compression moulding manufacturing process to produce composite truss sandwich cores. Variations of the braiding process have been used to produce composite truss beams. This includes the IsoTruss® [9]–[11] and the cylindrical lattice beam seen in [12]. Modifications of the filament winding manufacturing process have also been used to produce composite truss or frame type structures. This includes early versions of the Isotruss® [13] and the Anisogrid lattice technology developed in Russia in the 1980s [14], [15].

The patented Wrapped Tow Reinforced truss concept (WrapToR) [16] uses an adaptation of the filament winding process to produce composite truss beams. The process involves holding longitudinal members (referred to as chord members), which are typically premade composite tubes, on a rotating mandrel while wetted fibre tow is wound around them forming shear members. The process, depicted in Figure 1, produces trusses with all the fibres aligned with the member's respective primary loading directions, therefore maximising efficiency. The manufacturing process removes the need to assemble large numbers of parts as by winding wetted tow, shear elements are both created and co-bonded simultaneously. The concept is introduced by Woods et al. [17] in a study involving preliminary analysis, testing, and optimisation of the structures. During the study, testing to failure in torsional loading found the trusses to be prone to failure via compression buckling of the shear web members. Buckling of the members has also been highlighted as a critical failure mechanism in the mechanical testing of other composite truss concepts [12], [18], [19].

All previous work on this truss concept has investigated the original configuration seen in Figure 2a. In this configuration, the tow is wound in its as-purchased form where the fibres are spread out widthways. This produces shear web members that have a much lower second moment of area about one principle axis than the other. In this paper, a new configuration that is aimed at increasing the buckling resistance of the shear web members is investigated (Figure 2b). This previously untested technique involves twisting of the fibre tow during winding to produce shear web members with circular cross-sections. A circle has a constant second moment of area around the section, and crucially has the largest minimum second moment of area of any solid section for a given area. While this technique should improve the buckling resistance of the shear members it is possible that it could have detrimental effects on the bond strength at the truss nodes by reducing the bond area between the shear and chord members. Therefore, when assessing tow twisting as a method of improving the trusses structural efficiencies, both failure mechanisms should be considered.

In previous work on the WrapToR concept, trusses were manufactured by a “hand winding” technique in which the mandrel is rotated by an electric motor and tow is positioned onto the mandrel by hand. Within this study the design and build of a computer numerical controlled (CNC) truss winding machine is detailed. The development of this machine serves two functions: first, it allows manufacture of trusses with a consistent level of twist in the wound shear members, a task that is near impossible when hand winding. Second, it demonstrates the high level of automation achievable with this manufacturing process. Trusses manufactured using the machine are then tested to failure to investigate the effects of tow twisting on structural performance. Results of these tests are compared to predictions from a simple truss analysis tool. Finally, a comparison to commercially available composite tubes is conducted to demonstrate the potential benefits of the WrapToR truss configuration.

2 Manufacturing

2.1 Machine design and build

The truss winding machine was initially designed using computer aided design (CAD) software before purchase and assembly of the components. Low-cost and ease of modification were key drivers for the machine design. To achieve this, significant inspiration was drawn from the open-design movement which has grown rapidly in recent years allowing widespread production of homemade CNC machines. This led to a design where the supporting structures and linear rail are made from slotted aluminium extrusions, most of the mechanical parts are off-the-shelf, and 3D printed, or laser-cut plastic components were used where applicable. A CAD rendered image showing the layout of the machine with key components labelled is displayed in Figure 3. The machine has three mechanical degrees of freedom (DOF). Two of these degrees of freedom are inherent to any filament winding machine: a mandrel rotational axis and a longitudinal carriage translation axis. The third DOF is a rotation axis located on the tow delivery carriage that performs tow twisting.

The third DOF is the key difference between the truss winding machine and a conventional filament winder and results in a unique delivery carriage design. Conventional delivery carriages generally have assemblies of pulleys that spread the fibre tow [20]. Instead of spreading the fibres, the truss winder delivery carriage is designed to bundle the tow, by twisting it, to form circular section shear members. An image of the truss winder delivery head is shown in Figure 4. Here the entire tow spool, located at the rear of the carriage, is rotated using a motor, belt and pulley system. The rate of rotation is controlled to create a constant level of twist throughout the truss. The carriage design also features a spring and string frictional device for tow tensioning and a cast silicone resin bath with a through hole for tow impregnation.

Each machine DOF is driven by a stepper motor allowing precise control of absolute positioning without the need for external position feedback. Each motor is powered by a Toshiba TB6600 stepper driver. Relative motion of the three DOFs is controlled by an Arduino Mega microcontroller and the open source G-code interpreting software: GRBL. This set-up provides a low-cost and easily modifiable control system.

Another key component of the machine is the truss mandrel which holds the chord members in place during winding. The mandrel, seen in Figure 5, is constructed from three steel flat bars which are attached to a steel rod by several laser-cut acrylic ribs. The carbon pultruded rods that form the chord members of the trusses are then held onto the flat bars with acrylic clips. At the truss ends screws are attached to the clips which act as end stops allowing the tow to change direction once a pass of the carriage along the mandrel is completed.

2.2 Truss beam manufacture

The truss winding machine was used to produce truss beams for testing in three-point bending (Section 5). For the truss chord members, commercially available unidirectional pultruded carbon-epoxy tubes were used. The shear web was formed of Tenax IMS60 24K carbon fibre tow and SuperSap® CLV low viscosity bio-epoxy resin that was cured at room temperature. Tow feed-rate during winding was controlled at 2 m/min resulting in a winding time of 4 minutes and 40 seconds for the 1 m long trusses.

The aim of the study was to determine whether twisting the shear web tow to form a circular section shear web is beneficial to structural performance. As stated previously in Section 1, to test this hypothesis it is necessary to investigate how tow twisting effects both shear member buckling and the bond strength at the truss nodes. To probe each of these two failure mechanisms, trusses were manufactured in two sizes which create different relative amounts of loading in the shear webs and at the nodes. These truss sizes were selected using a combination of simple analysis (Section 4), engineering intuition, and experimental trial and error. The dimensions of the two chosen truss sizes are detailed in Table 1 and Figure 6. The first, larger truss size was selected to probe shear member buckling. It has a larger cross section with long, slender shear members which should be susceptible to buckling. Trusses of this size were manufactured at a length of 1 m and tested at a span of 792 mm, corresponding to twelve truss cells. The second truss size has half the section height and was selected to probe node debonding. Shear members in these trusses have a lower aspect ratio to reduce the likelihood of buckling, moving the critical region to the joints. A smaller pultrusion size was also selected for the chord members to reduce the bond area. Trusses of this size were manufactured at a length of 1 m, cut in half and tested at a span of 396 mm, corresponding to twelve truss unit cells. As the same number of large and small trusses were manufactured, cutting the small trusses in half resulted in double the number of small truss test samples, as is seen in Table 2.

For each truss size, samples with both straight-flat and twisted-circular shear web configurations were manufactured and tested. Trusses with straight-flat shear webs, referred to from hereon as “flat” samples, had a twist level of 0 twists per m. Those with twisted-circular shear webs, referred to as “twisted” samples, had a twist level of 30.3 twists per m. The two truss sizes and two shear web arrangements result in four test configurations. These configurations are given a label of two letters. The first letter corresponds to the truss size, either “L” for the larger size or “S” for the smaller. The second refers to the shear web twist level, either “F” for flat or “T” for twisted. The averaged mass per unit length of each configuration is given in Table 2. Twisting of the fibre tow was seen to have no significant effect on truss mass.

3 Microscopy

Shear member cross sections for both flat and twisted samples were investigated via optical microscopy to determine the effect of twisting on shear member shape and consolidation. Typical micrographs for each tow configuration are displayed in Figure 7. For the twisted tow samples (Figure 7b), near circular sections were observed. Section shapes in the flat samples were much less consistent with most samples resembling the micrograph in Figure 7a. In the micrographs displayed, significant void content is observed. This was common in all the obtained micrographs and is likely to stem from the lack of consolidation method employed during the manufacturing process. From the obtained optical micrographs, the principle second moments of area were determined by performing numerical integrations of 10 micrographs per tow configuration. These section properties were then used to predict how tow twisting would affect the buckling resistance of the members. The averaged results are displayed in Figure 8 where tow twisting is seen to reduce the variance of the section properties and increase the average minimum second moment of area by 56 %.

4 Analysis

During previous work, a structural analysis tool was developed for predicting truss deflections and member forces. The tool is based on a version of the direct stiffness method (DSM) that employs a two-force member assumption meaning members are assumed to experience only axial loadings [21], [22]. The tool is coded in MATLAB and its operation is further detailed in [17]. In this study the tool is used for two purposes. Firstly, the predicted truss deflections are compared to the experimental results to assess the code's accuracy. Secondly, the code is coupled with the classic Euler buckling formula to provide an analysis method for predicting truss failure due to shear web buckling. This was then applied to the larger section trusses to estimate the likely improvements in failure load when twisting the tow.

For buckling analysis, the DSM code was used to predict the internal loads within the truss members when the structure is externally loaded using the three-point bend test outlined in Section 5.1. Specifically of interest were the compressive loads within the shear members. These compressive loads were compared to critical buckling loads of the shear members which were determined using the Euler buckling formula:

$$P_{crit} = \frac{n\pi^2 EI}{L^2} \tag{1}$$

where the effective buckling length, L, was taken as half the shear member length, as is seen in Figure 6. The reasoning for this being that the repeating cross pattern of the trusses means that each shear member is bonded to one another shear member at its centre. When a truss is loaded in bending, for each shear web cross, one member will be in tension and one in compression. The tensile member therefore stabilises the compressive member at the cross over point, effectively halving the buckling length. The second moment of area, I, of the shear members were taken from the micrograph section integrations in Section 3. Youngs moduli, E, of the truss components were required for both the DSM analysis and the Euler buckling formula. Tensile moduli of the constituent components were determined experimentally by tensile testing of the pultrusion tubes (chord members) using ASTM D3916-08 [23] and the impregnated carbon tow (shear members) using ASTM D4018-17 [24]. Tensile and compressive moduli were assumed equal. Experimentally determined moduli are displayed in Table 3.

For the WrapToR truss shear members, the end condition factor, n, is not known meaning that the methodology described here could only be used to predict a range of truss failure loads. Due to the bonded attachments at the end of the shear members it was expected that the factor would lie between those for pinned-pinned ends (n=1) and fixed-fixed ends (n=4). The predicted three-point bending loads at which buckling would occur for different end condition factors are shown in Figure 9 for the L-F and L-T configurations. The highlighted range here shows that the L-F configuration is predicted to fail between 64 N and 257 N and the L-T between 103 N and 410 N. Assuming that the flat and twisted shear member configurations used would display the same end condition factor, the analysis predicts a 56 % increase in failure load when twisting the tow. This is equal to the measured increase in minimum second moment of area.

5 Experiment

5.1 Bending test

To investigate the effects of tow twisting on truss stiffness and strength, samples from each configuration were loaded to failure in a three-point bending test using the custom-built support rig in Figure 10. This rig was designed to test the trusses in a simply supported configuration. Load was applied by an Instron 8872 hydraulic test machine at a displacement rate of 4 mm/min with load readings recorded by a 5 kN load cell. Displacement was measured at the two lower central truss nodes using two laser sensors. Displacements of the rig at the truss support locations were also measured using

potentiometers to account for any deformation in the rig. Due to the novel configuration of the wound trusses, consideration into the load application method was necessary.

5.2 Selection of load application method

To determine the most appropriate method for introducing load into the trusses, an experimental investigation of different load introduction methods was conducted. Any loading method used for testing must not create excessive stress concentrations at loading points or supports that promote failure. Ideally the loading method would also apply load directly at the truss joints as this would allow direct comparison to the analysis tool

Three candidate loading configurations were selected and experimentally tested. Four small section trusses, two flat and two twisted, were tested to failure with each loading configuration. In each configuration load was applied at the locations shown in Figure 11 using 6mm steel rods. The average failure loads when using the different loading configurations are displayed in Figure 12. Here loading configuration 1 is seen to result in much lower failure loads. The samples tested with this method failed at the load application point due to debonding or failure of the upper chord member. When using this configuration, the load is applied to the most highly stressed region of the truss which appears to promote failure in that region. Configurations 2 and 3 displayed similar failure loads that were higher than those observed for configuration 1. For both methods no failure at the loading points or supports was observed. Configuration 3 however, does not have load applied directly at the nodes and therefore, loading configuration 2 was selected.

5.3 Comparison to commercially available CFRP tubes

In previous work by Woods et al.[17] low fidelity analysis work comparing the wound trusses to commercially available composite tubes showed increases in stiffness of up to two orders of magnitude for optimised WrapToR truss geometries. To investigate this experimentally, within this study two sizes of commercially available unidirectional pultruded CFRP tubes were tested to failure and compared to the S-T truss configuration. The tubes selected had similar mass per unit lengths to the small section trusses. These were a 7 mm and an 8 mm diameter tube, both of which had a wall thickness of 1 mm. Three tubes of each diameter were tested at the same span as the smaller section truss (396 mm) for direct comparison of stiffness and load carrying capability.

6 Results

6.1 Effects of tow twisting

The slender shear members of the larger trusses were susceptible to buckling resulting in all the large truss samples failing due to shear member buckling. Images of the buckled shear webs in both flat and twisted samples can be seen in Figure 14. The load-displacement graphs in Figure 13 show the structural responses of all the large section trusses. In all the graphs a stiffness reduction is observed at higher loadings, prior to failure. This non-linearity is caused by a bowing outwards of the shear members at higher loads. Bowing of the shear webs was more prominent and occurred at lower loads in the flat samples whose shear members had a lower minimum second moment of area. From the averaged results in Table 4 it is seen that twisting the tow improved load carrying capability of the larger section trusses by 51 %. Table 4 also shows average flexural rigidity, EI, which was estimated using the linear portion of the load displacement graphs and the classic deflection formula for a simply supported beam (Equation 2). The linear portions used were between 1.5-2.5 mm of deflection for the L-F configuration and 1.5-3.5 mm for the L-T configuration. Tow twisting was also seen to improve stiffness in the larger section trusses where flexural rigidity increased by 10 %. This increased stiffness is likely caused by the improved bending resistance of the circular section shear members. In Figure 13 a non-linearity is also witnessed in some samples at the start of testing which was caused by a slight unevenness of the samples on the test bed resulting in an initial bedding in phase.

$$\delta = \frac{Pl^3}{48EI} \quad (2)$$

For the smaller trusses the twisted configuration seems to display a small increase in stiffness and load carrying capability. However, statistical analysis of the test populations using the Welch's T-test [25] shows that no conclusive improvement can be drawn from the results. Investigation of the failure mechanisms of these samples found debonding of the shear web and chord members to occur in all samples. Figure 15 shows images of the most common failure mechanisms in the test samples, which for configuration S-F was debonding (Figure 15a), and for S-T was debonding coupled with chord compression failure (Figure 15b). As all the small samples failed due to debonding and no degradation in load carrying capability was observed in the twisted samples it can be concluded that for these samples tow twisting was not detrimental to node bond strength.

6.2 Analysis verification

In Table 5 the experimentally determined flexural rigidities for the twisted shear web truss configurations are compared to predictions made by the DSM analysis. Here for both truss sizes the DSM analysis is seen to significantly over-predict stiffness, particularly so in the larger section trusses. The analysis method used here is of low fidelity and assumes full two-force member behaviour in which each member of the truss only experiences axial loading. In reality the members are not free to rotate at the nodes and will therefore also experience bending moments. The analysis method also only models strains within the truss members and does not model strains within the joints. For the WrapToR configuration, where the truss members are fibre reinforced and the joints are not, strains at the joints may create a significant contribution to the overall displacement. It should also be noted here that due to the high stiffness of the trusses, the differences in deflections between the experimental and analytical results are only around 1 mm at failure load meaning that small experimental errors could be significant. Another possible source of this error may come from the bowing of the shear members. This is a non-linear effect caused by large deformations and will therefore not be captured by the linear analysis. Presence of this phenomenon may account for the increased error seen in the larger section trusses which have slenderer shear members and are more susceptible to bowing.

For both large section truss configurations, failure occurred within the range predicted by the buckling analysis. The experimentally determined improvement in failure load when twisting the tow was 51 % which is similar to the 56 % increase predicted by the analysis. Using the experimentally determined mean failure loads of the larger trusses which failed due to shear web buckling, the end condition factors were estimated at n=2.74 and n=2.66 for the flat and twisted shear members respectively.

6.3 Comparison to commercially available CFRP tubes

Results for testing of the pultruded CFRP tubes are displayed in Figure 16 alongside results for the small-twisted truss configuration. The results of these tests clearly show the potential benefits of the WrapToR configuration. Compared to the 7 mm tube the truss has 7 % more mass but achieves a 1006 % stiffness increase and a 181 % increase in load carrying capability. Compared to the 8 mm tube, the truss offers a mass saving of 9 %, a stiffness increase of 537 %, and a 133 % increase in load carrying capabilities. As both the tubes and the trusses are formed of unidirectional carbon fibre reinforced epoxy, this impressive increase in stiffness demonstrates how the WrapToR configuration uses geometry to drastically improve structural performance. It should be noted here that the truss configuration was in no way optimised for the loading scenario meaning that further improvements in structural efficiency are likely to be achievable with alteration of the truss geometry.

7 Conclusions and future work

This study aimed to investigate the effectiveness of a simple design technique for increasing the structural efficiency of WrapToR composite structures. The technique involved twisting of the carbon

fibre tow during the winding process to alter the shape of the shear members for improved buckling resistance. To achieve a consistent level of tow twisting a computer numerically controlled (CNC) winding machine was constructed and used to produce trusses with both twisted and non-twisted ("flat") shear members.

Inspection of the shear members cross section via optical microscopy found that tow twisting improved the consistency of the cross-section shape and increased minimum second moment of area by 56 %. Two truss sizes were tested to failure in three-point bending to investigate how tow twisting effects two possible failure mechanisms. In the larger truss size where shear member buckling was critical, twisting of the shear web tow increased truss load carrying capability by 51 % and truss stiffness by 10 %. This demonstrates how tow twisting increases the buckling resistance of the shear members. In the smaller truss size where node debonding was critical, no decrease in stiffness or failure load was observed, showing that tow twisting has no detrimental effect on the node bonds. These test results therefore confirm tow twisting to be beneficial to the structural efficiency of the WrapToR truss structures.

The experimentally determined deflections were compared to predictions from a previous developed structural analysis tool based on the direct stiffness method (DSM). The analysis tool was seen to significantly overpredict truss stiffness suggesting invalidity in the assumptions used by the method. This therefore prompts the need for development of higher fidelity analysis for more accurate prediction of structural response. Coupling of the analysis tool with Euler buckling formula demonstrated a method of predicting the truss loading at which shear member buckling may occur. Further work will also look at developing analysis tools to predict other likely truss failure modes, such as de-bonding and member material failure.

Experimental comparison of WrapToR trusses with conventional composite pultruded unidirectional tubes confirmed that at the length scales tested, the truss configuration provides large improvements in structural efficiency. Further work will investigate and demonstrate the technology at larger length scales to increase industrial applicability.

8 Acknowledgements

This work was supported by the Engineering and Physical Sciences Research Council through the EPSRC Centre for Doctoral Training in Advanced Composites for Innovation and Science [grant number EP/G036772/1].

9 Data statement

All the raw data used within this study is available for download at the University of Bristol data repository, data.bris, at https://doi.org/10.5523/bris.gtlkwtjtxtba2vbzo432xstso.

10 References

[1] M. F. Ashby, "Overview No. 92: Materials and shape," *Acta Metall. Mater.*, vol. 39, no. 6, pp. 1025–1039, 1991.

[2] P. M. Weaver and M. F. Ashby, "Material limits for shape efficiency," *Prog. Mater. Sci.*, vol. 41, no. 1–2, pp. 61–128, 1997.

[3] W. F. Chen and E. M. Lui, *Handbook of Structural Engineering*. New York, NY: CRC Press, 1997.

[4] "International Association for Shell and Spatial Structures (IASS) Working Group on Spatial Steel Structures. Analysis, design and realization of space frames," *Bulll. IASS*, vol. 84/85, no. XXV. p. 114, 1984.

[5] K. D. Potter, M. R. Wisnom, M. V Lowson, and R. D. Adams, "Innovative approaches to

composite structures," *Aeronaut. J.*, vol. 102, pp. 107–111, 1998.

[6] R. Schütze, "Lightweight carbon fibre rods and truss structures," *Mater. Des.*, vol. 18, pp. 231–238, 1997.

[7] J. Xiong, L. Ma, L. Wu, B. Wang, and A. Vaziri, "Fabrication and crushing behavior of low density carbon fiber composite pyramidal truss structures," *Compos. Struct.*, vol. 92, no. 11, pp. 2695–2702, 2010.

[8] W. Li, F. Sun, P. Wang, H. Fan, and D. Fang, "A novel carbon fiber reinforced lattice truss sandwich cylinder: Fabrication and experiments," *Compos. Part A Appl. Sci. Manuf.*, vol. 81, pp. 313–322, 2016.

[9] D. Jensen, M. Redford, and L. Francom, "On the structural efficiency of three-dimensional isogrid designs," *37th Struct. Struct. Dyn. Mater. Conf.*, pp. 1704–1710, 1996.

[10] D. H. A. D. Jensen, M J; Jensen, "Continuous Manufacturing of Cylindirical Composite Lattice Structures," in *International Conference on Textile Composites (TEXCOMP10)*, 2010.

[11] D. W. Jensen, "Using External Robots Instead of Internal Mandrels to Produce Composite Lattice Structures," in *International Conference on Textile Composites (TEXCOMP10)*, 2010.

[12] A. Gurley, D. Beale, R. Broughton, and D. Branscomb, "The Design of Optimal Lattice Structures Manufactured by Maypole Braiding," *J. Mech. Des.*, vol. 137, no. 10, p. 101401, 2015.

[13] T. Weaver and D. W. Jensen, "Mechanical characterization of a graphite/epoxy IsoTruss," *Jorunal Aerosp. Eng.*, vol. 13, no. January, pp. 23–35, 2000.

[14] V. V. Vasiliev, V. A. Barynin, and A. F. Rasin, "Anisogrid lattice structures – survey of development and application," *Compos. Struct.*, vol. 54, no. 2–3, pp. 361–370, 2001.

[15] V. V. Vasiliev and A. F. Razin, "Anisogrid composite lattice structures for spacecraft and aircraft applications," *Compos. Struct.*, vol. 76, no. 1–2, pp. 182–189, 2006.

[16] B. Woods, B. Otto Berry, and V. Bohdan Stavnychyi, "Continuous Wound Composite Truss Structures," US2013/0291709, 2013.

[17] B. K. S. Woods, I. Hill, and M. I. Friswell, "Ultra-efficient wound composite truss structures," *Compos. Part A Appl. Sci. Manuf.*, vol. 90, pp. 111–124, 2016.

[18] S. Ju, D. Z. Jiang, R. A. Shenoi, and J. Y. Xiao, "Flexural properties of lightweight FRP composite truss structures," *J. Compos. Mater.*, vol. 45, no. 19, pp. 1921–1930, 2011.

[19] M. E. Rackliffe, D. W. Jensen, and W. K. Lucas, "Local and global buckling of ultra-lightweight IsoTruss structures," *Compos. Sci. Technol.*, vol. 66, no. 2, pp. 283–288, 2006.

[20] S. Peters, *Composite FIlament Winding*. ASM Internationl, 2011.

[21] J. S. Przemieniecki, *Theory of Matrix Structural Analysis*. 1968.

[22] H. Kardestuncer, *Elementary Matrix Analysis of Structures*. New York, NY, 1974.

[23] ASTM, "ASTM D3916-08: Standard Test Method for Tensile Properties of Pultruded Glass-Fiber-Reinforced." .

[24] ASTM, "ASTM D4018-17: Standard Test Methods for Properties of Continuous Filament Carbon and Graphite Fiber Tows." .

[25] N. Salkind, *Encyclopedia of Research Design*. California, United States: SAGE Publications, Inc., 2010.

11 Figures

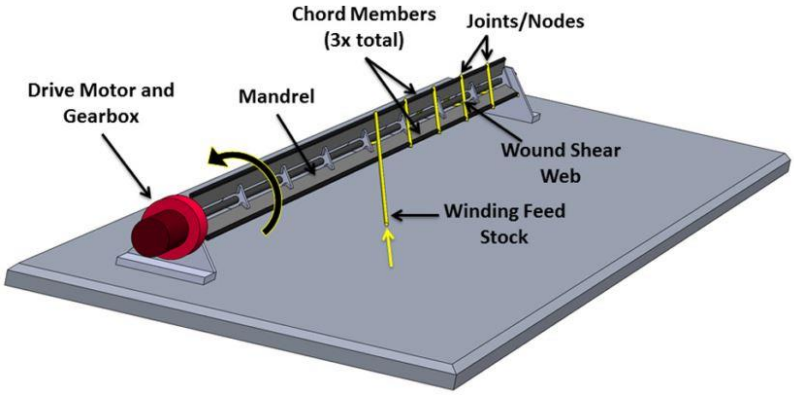

Figure 1. Schematic of WrapToR winding process. Reproduced from [17].

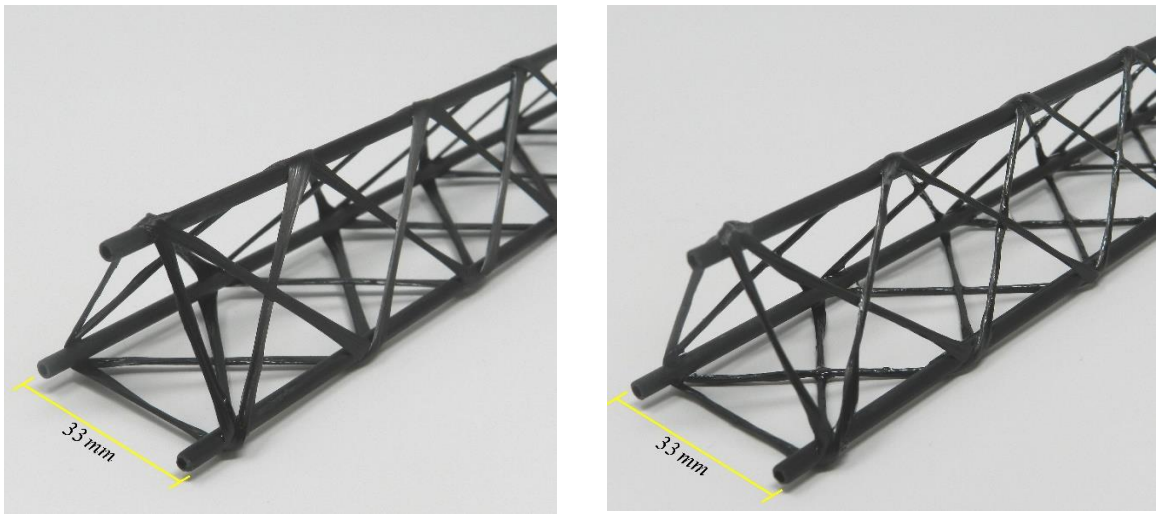

Figure 2: a) Previous WrapToR truss design; b) Truss with twisted tow shear web.

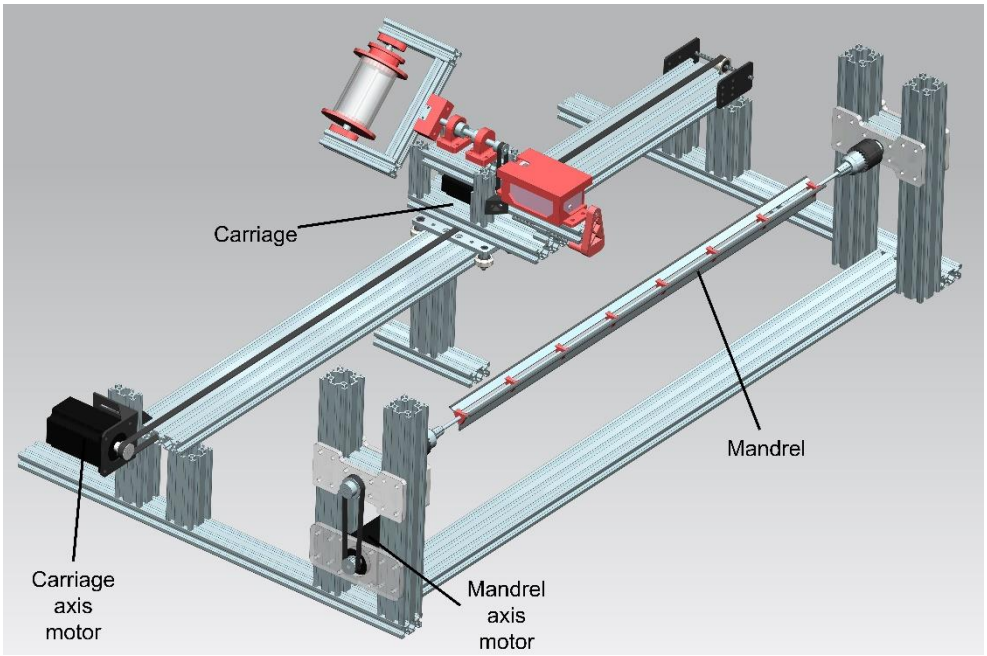

Figure 3: CAD model image of WrapToR truss winding machine.

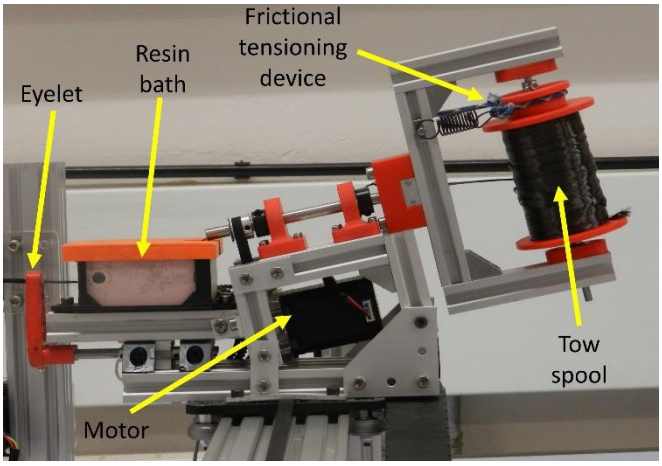

Figure 4: Tow delivery carriage.

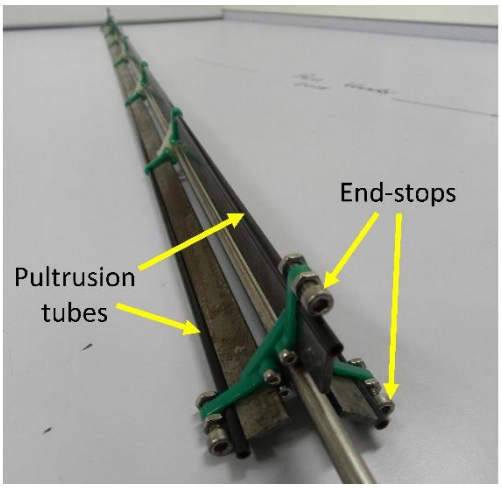

Figure 5: Truss mandrel.

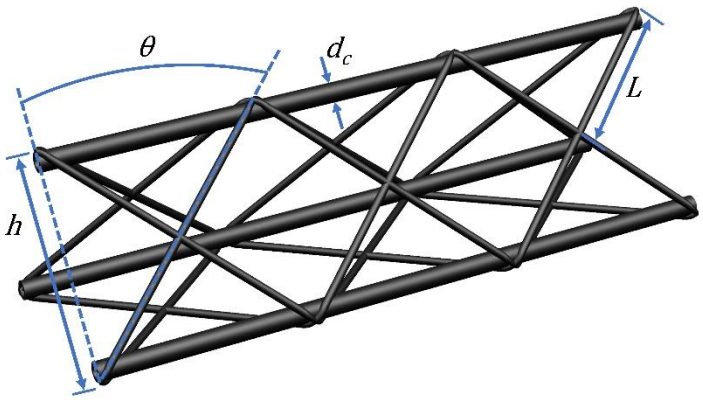

Figure 6: Truss geometry definition.

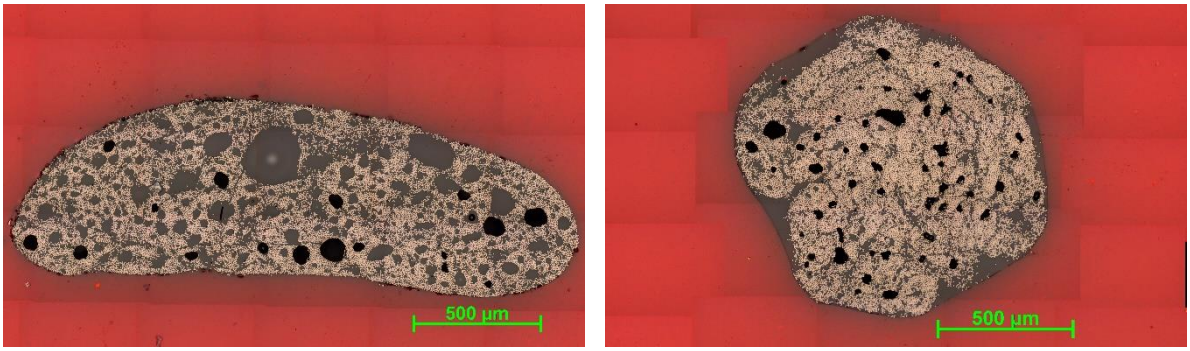

Figure 7: Micrographs of truss shear member cross-section for shear web configuration: a) flat; b) twisted.

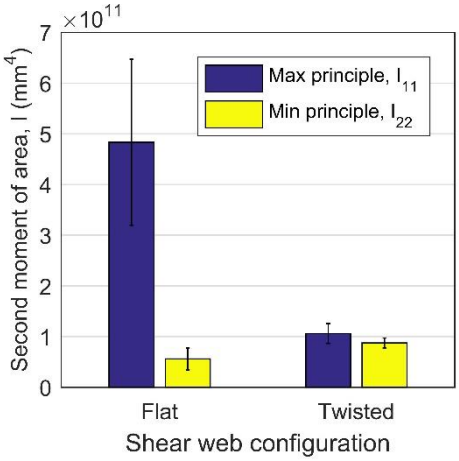

Figure 8: Average principle second moments of area for shear web configurations.

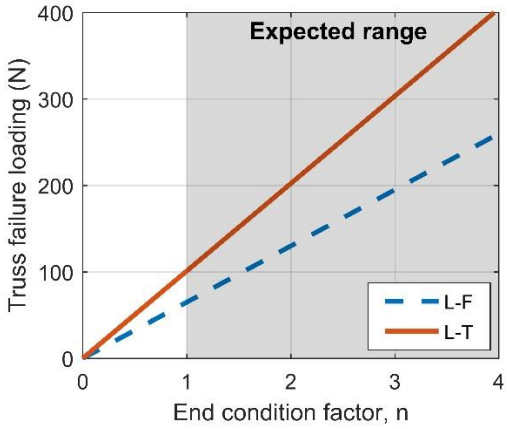

Figure 9: Predicted failure load due to shear member buckling over range of end condition factors. Large section samples only.

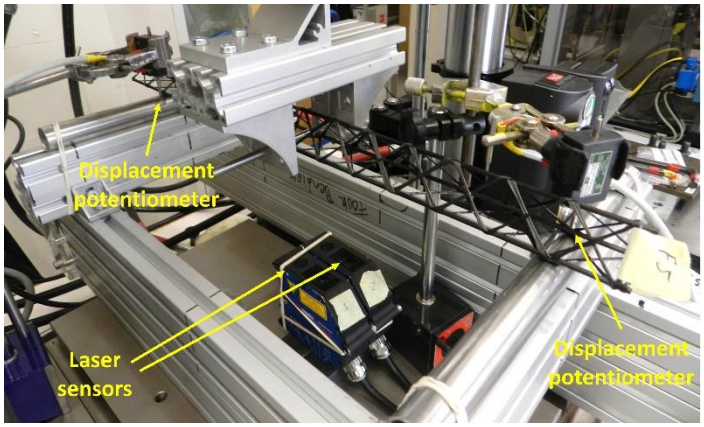

Figure 10. Three-point bend test set-up.

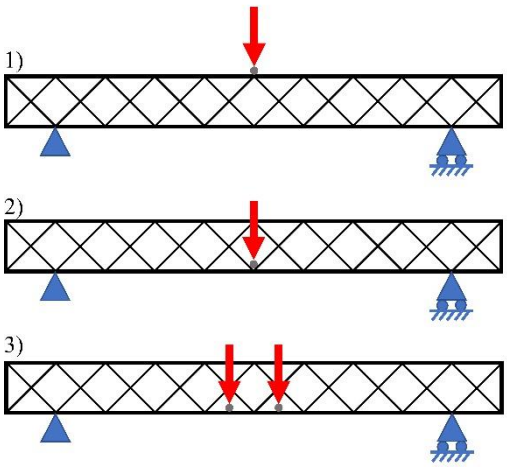

Figure 11: Candidate loading configurations.

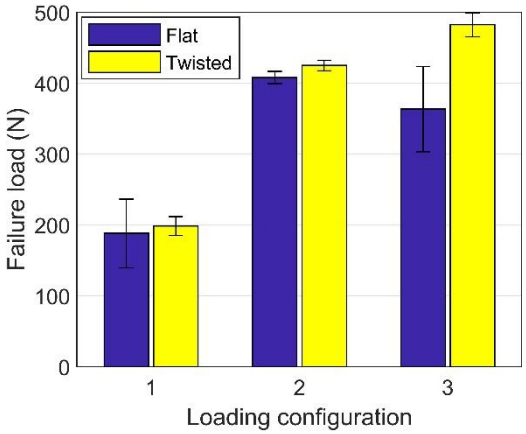

Figure 12: Average failure load for different loading configurations. (Error bars denote 1 standard deviation)

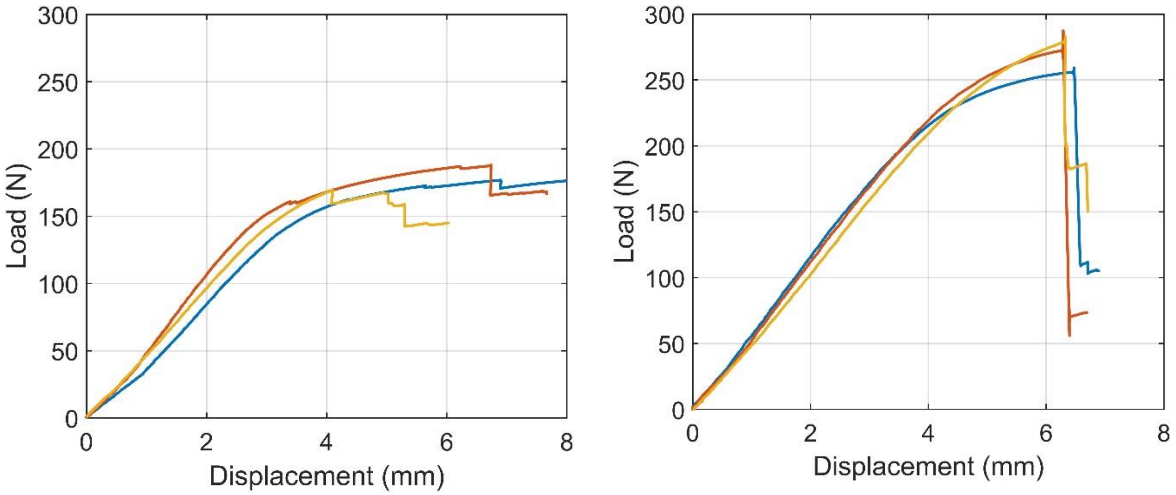

Figure 13: Load displacement graphs for large section trusses of the two configurations: a) L-F; b) L-T.

Figure 14: Failure in large section truss configurations: a) L-F; b) L-T.

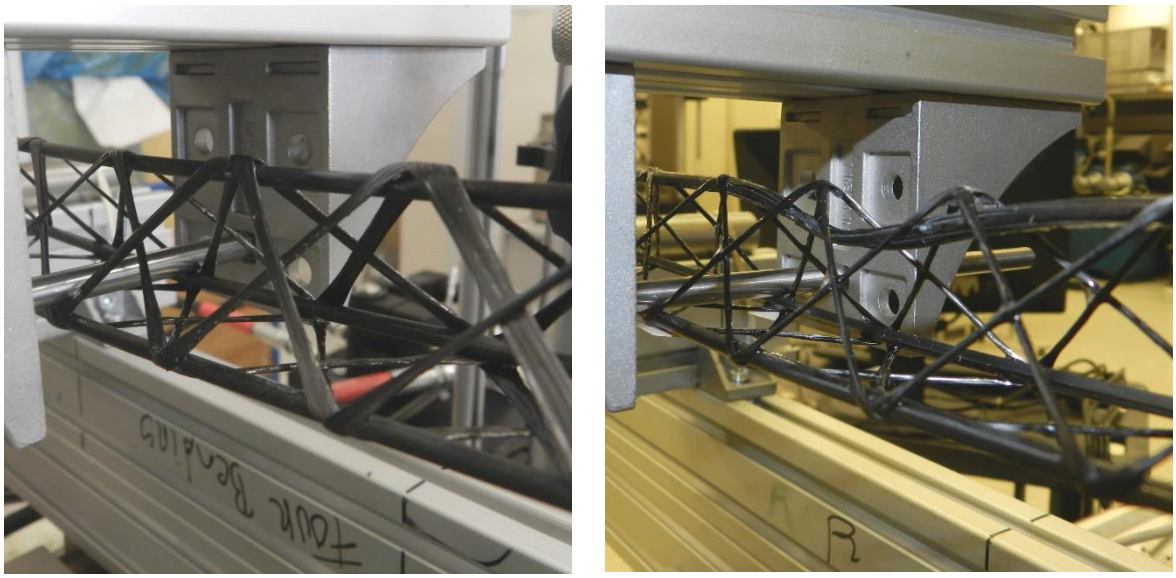

Figure 15: Failure in small section truss configurations: a) S-F: debonding; b) S-T: debonding and chord failure.

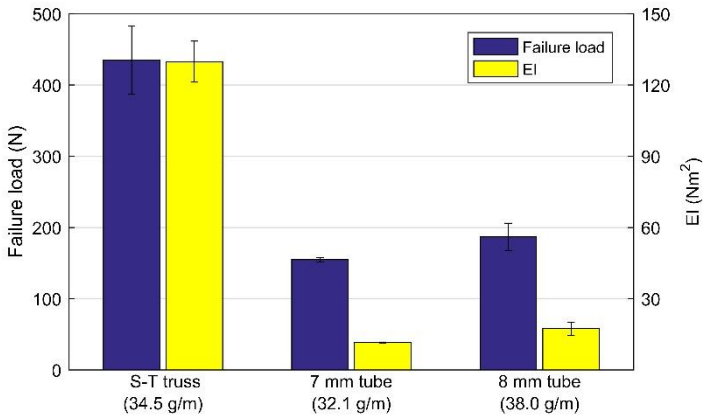

Figure 16: Failure loads and flexural rigidity of small-twisted truss configuration and pultruded tubes. (Error bars denote 1 standard deviation).

12 Tables

Table 1: Dimensions of selected truss sizes.

Geometric property	Symbol	Units	Truss size	
			Large	Small
Truss height	h	mm	66	33
Chord tube diameter	d_c	mm	4	3
Chord tube wall thickness	t_w	mm	0.5	0.5
Winding angle	θ	deg	45	45
Shear member buckling length	L	mm	23.3	46.7

Table 2: Average test sample mass.

Configuration ID	Number of samples	Mass per unit length (g/m)	
		Mean	Standard deviation
Large Flat (L-F)	3	42.2	0.8
Large Twisted (L-T)	3	41.2	0.4
Small Flat (S-F)	6	33.5	0.8
Small Twisted (S-T)	6	34.2	0.6

Table 3: Moduli of truss constituent components.

Truss component	Member	Youngs modulus (MPa)
Pultruded CFRP tube	Chord	137.6
Impregnated CFRP tow	Shear	107.8

Table 4: 3-point bend test results for the truss configurations.

Configuration	Flexural rigidity (Nm^2)		Failure load (N)	
	Mean	CV (%)	Mean	CV (%)
L-F	528.9	6.3	178.3	5.2
L-T	579.4	1.5	269.0	4.4
S-F	121.5	3.9	407.8	8.6
S-T	129.9	6.6	434.9	11.0

Table 5: Comparison of experimentally and analytically determined flexural rigidities for twisted shear web trusses.

Configuration	Flexural rigidity (Nm^2)		
	Experimental	Analytical	% error
S-T	128.3	172.0	34.1
L-T	594.5	920.9	54.9